Chapter 6

The Use of MODIS Images to Quantify the Energy Balance in Different Agroecosystems in Brazil

Antônio Heriberto de Castro Teixeira,
Janice F. Leivas, Carlos C. Ronquim and
Gustavo Bayma-Silva

Additional information is available at the end of the chapter

http://dx.doi.org/10.5772/intechopen.72798

Abstract

Sugarcane (SC) is expanding over coffee (CO), while both crops have replaced the natural vegetation (NV) in the northeastern side of São Paulo (SP) state, Southeast Brazil. Under these dynamic land-use changes, geosciences are valuable tools for evaluating the large-scale energy and mass exchanges between the vegetation and the lower atmosphere. For quantification of the energy balance components in these mixed agroecosystems, MODIS images were used throughout the Simple Algorithm for Evapotranspiration Retrieving (SAFER) algorithm, during the year 2015 in the main sugarcane- and coffee-growing regions of the state. Regarding, respectively, sugarcane, coffee, and natural vegetation, the fractions of the net radiation (Rn) used as latent heat flux (λE) were 0.68, 0.87, and 0.77, while the corresponding ones for the sensible heat (H) fluxes were 0.27, 0.07, and 0.16. Negative H values were noticed from April to July, because of heat advection raising λE values above Rn, but they were more often in coffee than in sugarcane. It was concluded that sugarcane crop presented lower evapotranspiration rates, when compared with coffee, which could be an advantage under the actual water scarcity scenario. However, sugarcane replacing natural vegetation means environmental warming, while the land use changes promoted by coffee crop represented cooling conditions.

Keywords: safer, land use changes, latent heat flux, sensible heat flux, soil heat flux

1. Introduction

Sugarcane (SC) (*Saccharum officinarum*) and coffee (CO) (*Coffea arabica* L.) crops are expanding in the northeastern side of the São Paulo (SP) state, Southeast Brazil. The first one is an annual crop, while the second one is a perennial crop, but both are replacing the natural vegetation (NV), composed by a mixture of Savannah and Atlantic Coastal Forest species. However,

sugarcane is also replacing the coffee areas [1], as consequences of both sugar and alcohol explorations, but also by stimulating renewable energy use [2].

The negative effects of the sugarcane expansion could be more serious when compared with those from the fossil fuel exploration, regarding greenhouse gas emissions [3, 4]. Aiming bio-energy production, a crop has to grow fast presenting high yield, but its energy output must exceed fossil fuel energy input. Considering these issues, sugarcane is a good candidate for energy crop [5]. However, its expansion could affect the large-scale energy balance further influencing the carbon cycle [6–8]. Anderson-Teixeira et al. [9] have reported energy balance alterations because of sugarcane expansion.

Under land-use and climate change conditions, the use of tools for quantifying the large-scale energy balance components is relevant for supporting policy planning and decision-makings about the water resources. The difficulties of measuring and analyzing these components throughout only field measurements highlighted the importance of coupling remote sensing and weather data, which have been successfully done in commercial crops under different environmental conditions [3, 10].

Several algorithms have been developed for acquiring the large-scale energy balance components. The Simple Algorithm for Evapotranspiration Retrieving (SAFER) is applied in this chapter in sugarcane and coffee crops comparing the results with those for natural vegetation. The algorithm was developed and validated in Brazil based on simultaneous field radiation and energy balance data from experiments and remote sensing under strongly water and vegetation contrasting conditions [11, 12].

Having cropland masks available, the energy balance components are analyzed in these mixed agroecosystems by the coupling MODIS images and weather data. The results may subsidize policies for a rational sugarcane and coffee water managements, being the analyses very useful under the actual scenario of water competitions between these crops and other sectors in the Southeast Brazil, as consequences of both climate and land use changes.

2. Materials and methods

2.1. Study region, crops, and agrometeorological data

Figure 1 shows the location of the study region in the northeastern side of São Paulo state, Southeast Brazil, together with the cropland masks and the agrometeorological stations used for the weather data gridding processes.

The agroecosystems are constituted by sugarcane (SC) and coffee (CO) interspaced with natural vegetation (NV). This last class is a mixture of Savannah and Atlantic Coastal Forest species. Some of the areas before occupied by coffee are nowadays being replaced by sugarcane crop.

The sugarcane areas present two well-defined seasons: the first one rainier and hotter and the other one drier and colder. According to Cabral et al. [13], the long-term maximum rainfall occurs in December (274 ± 97 mm month^{-1}), and the minimum one is between July and August

http://dx.doi.org/10.5772/intechopen.72798

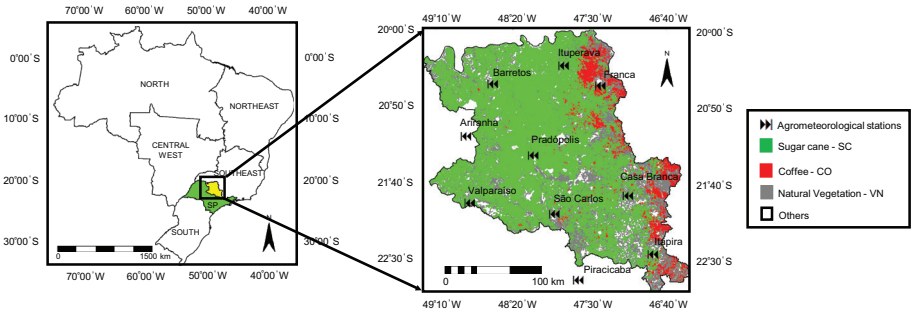

Figure 1. Location of the study region inside the northeastern side of the São Paulo state, Southeast Brazil, together with the cropland masks and the agrometeorological stations used for the weather data gridding processes.

(27 ± 34 mm month^{-1}); the annual value is 1517 ± 274 mm yr.$^{-1}$. The mean air temperatures in January and July are, respectively, 24 and 19°C, and the annual average is 22°C.

The sugarcane phases may be divided into four [14]: Phase 1: Germination and establishment, from January to February, are influenced by soil moisture, soil temperature, and soil aeration, denoting activation and subsequent sprouting of the vegetative bud. Phase 2: Tillering is influenced by variety, solar radiation, air temperature, soil moisture, and fertilization, starting from around 40 days after the initiation of the growing cycle and may last up to 120 days (February–April). Phase 3: Grand growth is from 120 days after the starting of the growing cycle lasting up to 270 days in a 12-month crop (May–September). Both high soil moisture and solar radiation levels favor better cane elongation during this phase. Phase 4: Ripening and maturation are characterized by slower growth activity, lasting for about 3 months starting from 270 to 360 days after the growing cycle initiation (September–December). High solar radiation levels and low soil moisture conditions are favorable during this last phase [15].

The coffee crop concentrates at the right side of the study area (see **Figure 1**). The region presents also a rainy season and a dry winter somewhat similar to the sugarcane areas; however, due to higher altitudes, between 700 and 1100 m, the long-term annual air temperature ranges are lower, from 18 to 20°C [16].

The coffee crop in Brazil, differently from sugarcane, which completes its average growing cycle in 12 months, takes 2 years for its all crop stages. Six coffee phases are considered, starting in September of each year [17, 18]: Phase 1: Vegetation with bud formation, during 7 months, is normally from September to March. Phase 2: Vegetation is between April and August, when the transformation of the vegetative to reproductive buds occurs, when at the end of this phase, from July to August, the plants enter in relative dormancy stage. Phase 3: Flowering and grain expansion are normally from September to December. Phase 4: Grain formation is normally from January to March, when water stress can be detrimental to the grain development. Phase 5: Grain maturation. Moderate water stress can benefit the grains. Phase 6: Senescence and death of the non-primary productive branches generally occur in July and August. In this last stage, the self-pruning process represented by senescence occurs, when the productive branches wither and die, limiting plant development.

2.2. Large-scale energy balance modeling

For the large-scale modeling, the MODIS images were used during the year 2015 together with 10 agrometeorological stations from the National Meteorological Institute (INMET) in the study area, considering the cropland classes. Weather data were used to calculate the reference evapotranspiration (ET0) by the Penman-Monteith method [19]. The weather input modeling parameters, global solar radiation (RG), air temperature (T_a), and ET_0 were up scaled for the 16-day period of the MODIS MOD13Q1 reflectance product (spatial resolution of 250 m) and gridded by using the moving average method generating pixels with the same spatial resolution as the satellite images.

Figure 2 shows the steps for modeling the energy balance throughout the SAFER algorithm with the MODIS MOD13Q1 product.

Following **Figure 2**, the surface albedo (α_0) was estimating according to Valiente et al. [20]:

$$\alpha_0 = a + b\alpha_1 + c\alpha_2 \quad (1)$$

where α_1 and α_2 are the reflectances from the bands 1 and 2, respectively, and a, b, and c are regression coefficients, considered as 0.08, 0.41, and 0.14, obtained under different Brazilian vegetation types and distinct hydrological conditions [10].

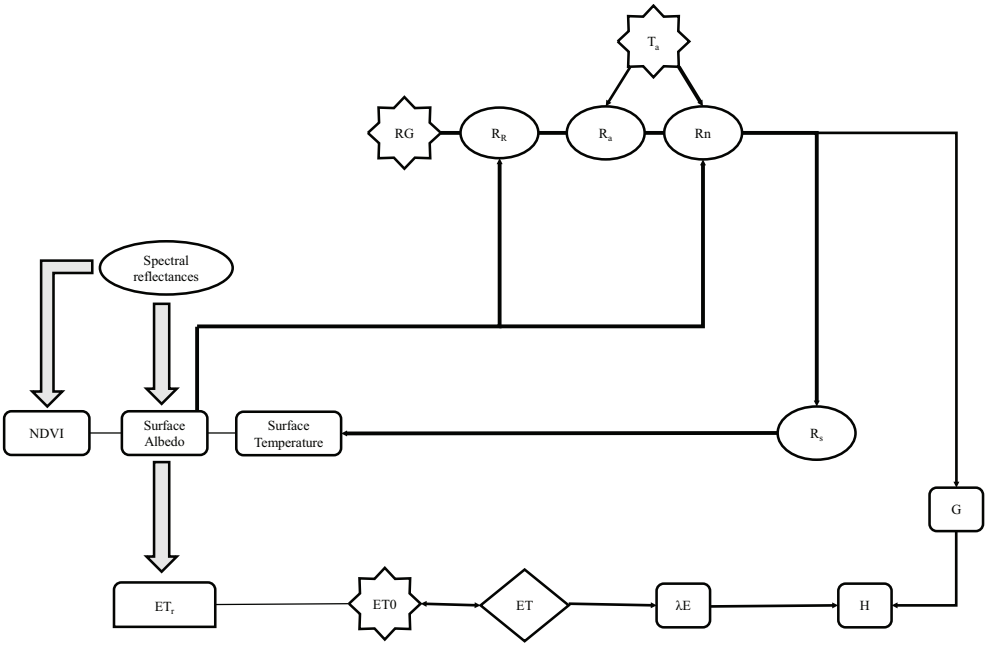

Figure 2. Flowchart for modeling the energy balance throughout application of the SAFER algorithm to the MODIS MOD13Q1 product.

The normalized difference vegetation index (NDVI) is a measure of the amount of vegetation at the surface:

$$NDVI = \frac{\alpha_2 - \alpha_1}{\alpha_2 + \alpha_1} \quad (2)$$

The reflected solar radiation (R_R) was estimated as

$$R_R = \alpha_0 RG \quad (3)$$

The longwave atmospheric radiation (R_a) was calculated by applying the Stefan-Boltzmann low:

$$R_a = \sigma \varepsilon_A T_a \quad (4)$$

where ε_A is the atmospheric emissivity and σ is the Stefan-Boltzmann constant (5.67×10^{-8} W m^{-2} K^{-4}).

The parameter ε_A was calculated according to Teixeira et al. [21]:

$$\varepsilon_A = a_A (-\ln \tau)^{b_A} \quad (5)$$

where τ is the shortwave atmospheric transmissivity calculated as the ratio of R_G to the incident solar radiation at the top of the atmosphere and a_A and b_A are the regression coefficients 0.94 and 0.10, respectively.

Net radiation (Rn) can be described by the 24-hour values of net shortwave radiation, with a correction term for net longwave radiation [22]:

$$Rn = (1 - \alpha_0)RG - a_L \tau \quad (6)$$

where a_L is the regression coefficient of the relationship between net longwave radiation and τ on a daily scale.

Because of the thermal influence on longwave radiation via the Stephan-Boltzmann equation, a_L coefficient from Eq. (6) was correlated with the 24-hour T_a [11]:

$$a_L = dT_a - e \quad (7)$$

where d and e are the regression coefficients found to be 6.99 and 39.93, respectively.

Having estimated R_R, R_a, and Rn, the emitted surface longwave radiation (R_s) was acquired as residue in the radiation balance equation:

$$R_S = RG - R_R + R_a - Rn \quad (8)$$

Then, the surface temperature (T_0) was estimated by the residual method [22]:

$$T_0 = \sqrt[4]{\frac{R_s}{\sigma \varepsilon_s}} \tag{9}$$

where the surface emissivity (ε_S) was estimated as follows [22]:

$$\varepsilon_S = a_S(\ln \text{NDVI}) + b_s \tag{10}$$

and a_S and b_S are the regression coefficients 0.06 and 1.00, respectively.

The SAFER algorithm is used to model water indicator represented by the ratio of the actual to the reference evapotranspiration (ET_r) based on the input remote sensing parameters, which is then multiplied by the 24-hour ET_0 values to estimate the daily ET large-scale rates which in turn are transformed into latent heat fluxes (λE):

$$ET_r = \left\{ \exp\left[f + g\left(\frac{T_0}{\alpha_0 \text{NDVI}} \right) \right] \right\} \frac{ET\,0_{yr}}{5} \tag{11}$$

where f and g are the original regression coefficients, 1.8 and −0.008, respectively. The correction factor ($ET0_{yr}/5$) is applied, $ET0_{yr}$ being the annual grids of reference evapotranspiration for São Paulo state in the year 2015 and 5 mm is the ET_{0yr} value for the period of the original modeling in the Northeast Brazil [21].

For soil heat flux (G), the equation derived by Teixeira [12] was used:

$$\frac{G}{R_n} = a_G \exp(b_G \alpha_0) \tag{12}$$

where the regression coefficients a_G and b_G are 3.98 and −25.47.

The sensible heat flux (H) is acquired as residue in the energy balance equation:

$$H = R_n - \lambda E - G \tag{13}$$

3. Results and discussion

3.1. Thermohydrological conditions and crop stages

The driving weather variables for the surface energy balance are R_G, T_a, precipitation (P), and ET_0. They are presented in **Figure 3** on a 16-day time scale in terms of day of the tear (DOY), during 2015 as average pixel values for each agroecosystem class: sugarcane (SC), coffee (CO), and natural vegetation (NV).

Among the four weather parameters, P was the most variable along the year with the largest values occurring during the first and the last 3 months. The high-moisture conditions in the root zones during these periods affect the energy balance, increasing the latent heat fluxes (λE) for all agroecosystems. The rainfall annual totals were 1253, 1277, and 1245 mm yr^{-1} for the sugarcane (SC), coffee (CO), and natural vegetation (NV) with the range of standard

deviation (SD) staying between 11 and 12 mm yr^{-1}. These values are below the historical value of the study area, and they were not well distributed along the year. A period from July to October, with several rainfall 16-day values bellow 10 mm, was noticed for all analyzed agroecosystems. The short rainfall amounts occurred from Phase 3 to Phase 4 of the generalized sugarcane growing cycle, which should have caused some water deficit, when its water requirements are high. Cabral et al. [13] reported a 13% of sugarcane biomass reduction in relation to the regional average in São Paulo state, Brazil, because of the lower water availability observed during the initial 120 days of cane regrowth. For rainfed sugarcane crop, a well-distributed growing season total precipitation between 1100 and 1500 mm is considered adequate. However, the P dropping during Phase 3 should have caused some water deficit, when the crop water requirements are high, further affecting the energy partition, by reducing leaf area and the number of tillers and leaves per stalk [23]. During Phase 4, rains are not desirable for sugarcane, because they lead to poor juice quality [15], and then the high amounts at the end of the year, coinciding with this phase, were not favorable.

Taking into account the ET_0 values, one can see two atmosphere demand peaks with the smallest one happening at the middle of the year, however, with lower differences among the agroecosystems when compared with precipitation. The corresponding ET_0 annual values were 1321, 1297, and 1293 mm yr^{-1} for the sugarcane (SC), coffee (CO), and natural vegetation (NV) but with small SD from 3 to 4 mm yr^{-1}. The shortest ET_0 values in the middle of the year,

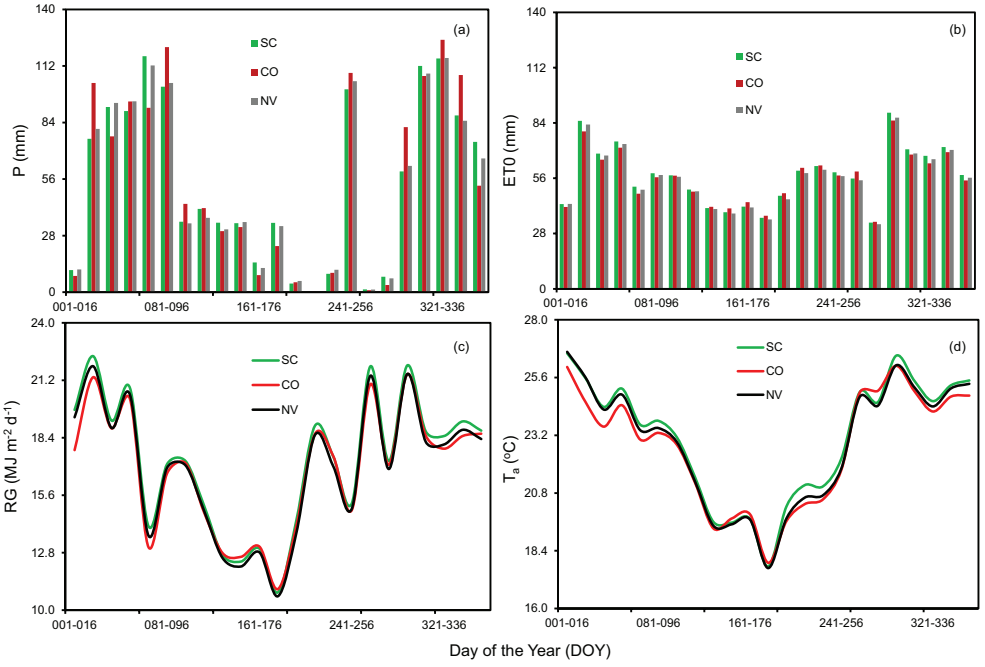

Figure 3. Average 16-day values for the weather variables during 2015 in areas with sugarcane (SC), coffee (CO), and natural vegetation (NV) in terms of day of the year (DOY), located at the northeastern side of São Paulo state, Brazil. (a) Precipitation (P), (b) reference evapotranspiration (ET_0), (c) incident global solar radiation (R_G), and (d) air temperature (T_a).

from May to July, coincide with the sugarcane Phase 3, favoring cane elongation reduction during this phase.

In relation to R_G and T_a, the differences among the agroecosystems were smaller than those for P and ET_0, with average annual values around 17 MJ m^{-2} day^{-1} and 23.0°C, respectively. Then, the highest atmosphere demands in sugarcane could be probably attributed to low air humidity and/or high wind speed conditions.

The thermohydrological conditions also strongly affect the coffee crop stages [17]. As the growing cycle takes 2 years, some coffee phases will coexist. Rainfall should be well distributed for good yield. At the start of the year, for the period involving Phases 1 and 4, there was only a 16-day (DOY 001–016) period with P lower than 10 mm in January. In Phase 2 rainfall is important for the transformation of the vegetative to reproductive buds. During this period, P declined until values close to zero at the end of July (DOY 209–224). In Phase 3 (September–November), some water stress is desirable, as the main flowering happens during a period of water stress following by good water availability. However, only two 16-day periods with low rainfall amounts are verified from September to October (DOY 257–288). In Phase 4, water stress may wilt the fruits, but only during the period from DOY 001 to 016 the rainfall amount was low, bellow 10 mm. In Phase 5 the water requirements declined, and some water deficit during this phase could have favored the coffee plant growth. The period with low rainfall amounts from May to June was also inside this phase.

Conditions of low R_G and ET_0 levels from May to August coincided with low P amounts, thus reducing water consumption in coffee areas. Air temperature (T_a) regulates the vegetative growth and reproductive buds, being high values associated with water deficit during booming the reason for flower abortion and growth reduction [23]. However, the higher values, above 23°C, occurred under conditions of good rainfall availability.

3.2. Agroecosystem energy balances

Figure 4 shows the composed average net radiation (Rn) values for sugarcane (SC), coffee (CO), and natural vegetation (NV) agroecosystems, during the year 2015, inside the northeastern side of São Paulo (SP) state, Southeast Brazil.

The lowest Rn pixel values are in the middle of the year, when reached close to 6.0 MJ m^{-2} d^{-1}, while the maximum ones were above 10 MJ m^{-2} d^{-1}. All ecosystems averaged 9.0 MJ $m^{-2}d^{-1}$; however, with small spatial variation, one can see from the SD values with range from 0.3 to 1.5 MJ m^{-2} d^{-1}. The highest end of this range was for the coffee (CO) class, in DOY 225–240 (August), period of the year coexisting plants inside Phases 2 and 6.

To see the energy availability in detail for the different agroecosystems along the year, **Figure 5** presents the Rn average values (a) and their fractions to RG (b) for sugarcane (SC), coffee (CO), and natural vegetation (CO), during the year 2015, in the northeastern side of São Paulo (SP) state, Southeast Brazil.

The strong dependence of Rn on RG is clear for all analyzed agroecosystems (see **Figures 3c** and **5a**). The Rn trends for the sugarcane (SC) and natural vegetation (NV) classes were similar, but values for coffee (CO) were a little lower, at the start and at the end of the year, during

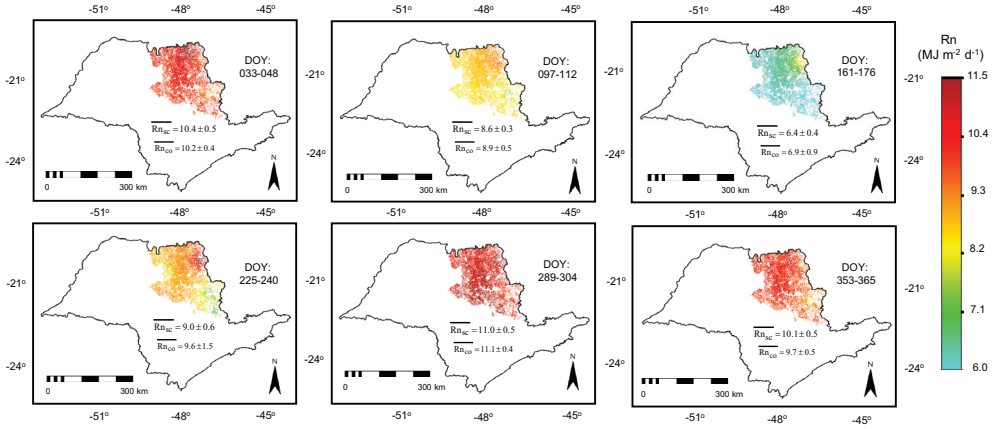

Figure 4. Composed net radiation (Rn) average values for sugarcane (SC), coffee (CO), and natural vegetation (NV) agroecosystems, during the year 2015, inside the northeastern side of São Paulo (SP) state, Southeast Brazil. The over bars mean averages showed together with standard deviations (SD).

Phases 1 and 4 of coffee plants. However, at the middle of the year, CO values were higher, when the plant stages were in mixed stages of the Phases 2, 5, and 6.

Regarding the ratio Rn/RG (**Figure 5b**), the higher mean pixel values were for the coffee (CO) class, mainly in the middle of the year. The values ranged from 0.49 to 0.55, from 0.50 to 0.57, and from 0.50 to 0.56, for, respectively, the SC, CO, and NV agroecosystems. The average annual Rn/RG of 50–55% is in agreement with field measurements in fruit crops and natural vegetation in the Northeast Region of Brazil [11] and with studies involving other distinct agroecosystems around the world [24, 25]. These results of similarities with national and international studies give confidence to the large-scale remote sensing methods tested here by coupling the MOD13Q1 product and agrometeorological stations.

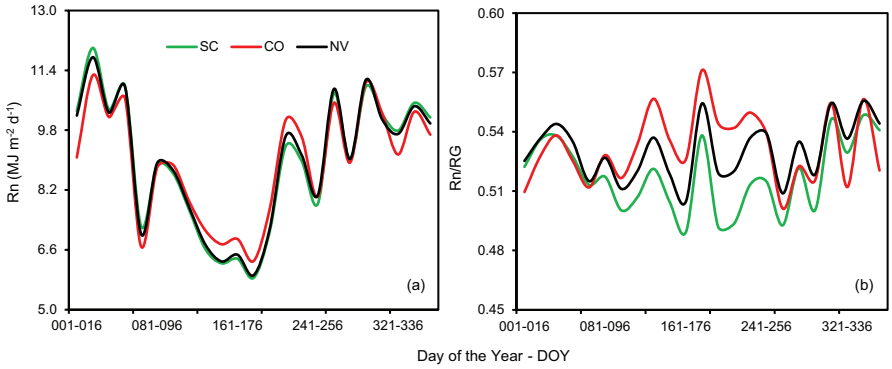

Figure 5. Daily net radiation (Rn) and their ratios to global solar radiation (RG) for sugarcane (SC), coffee (CO), and natural vegetation (NV) agroecosystems, during the year 2015, in the northeastern side of São Paulo (SP) state, Southeast Brazil. The over bars mean averages showed together with standard deviations (SD).

The composed latent heat flux (λE) values in the sugarcane (SC), coffee (CO), and natural vegetation (NV) agroecosystems, during the year 2015 inside the northeastern side of São Paulo (SP) state, Southeast Brazil, are shown in **Figure 6**.

Much more distinct of both λE and SD values among the agroecosystems are noticed than in the case of Rn, with λE ranging from close to zero to becoming higher than 13 MJ m^{-2} d^{-1}. The lowest values were for the sugarcane (SC) class, with an average λE of 6.1 ± 2.2 MJ m^{-2} d^{-1}, followed by natural vegetation (NV), 6.9 ± 1.8 MJ m^{-2} d^{-1}, and coffee (CO) with the highest average of 7.8 ± 1.8 MJ m^{-2} d^{-1}. Besides the lowest λE, the SC class presented also the largest spatial variation. Considering all agroecosystems, the highest and the lowest λE rates were, respectively, in January and at the end of October.

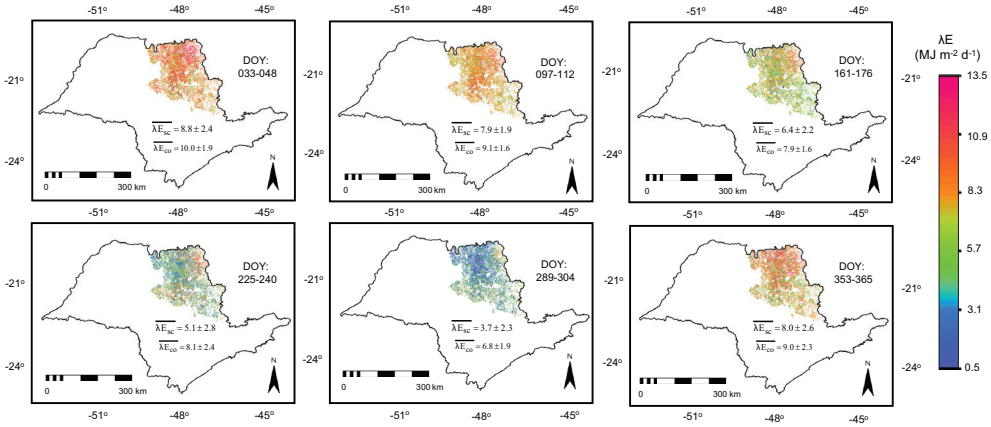

Figure 6. Composed latent heat flux (λE) values for the sugarcane (SC), coffee (CO), and natural vegetation (NV) agroecosystems, during the year 2015, inside the northeastern side of São Paulo (SP) state, Southeast Brazil. The over bars mean averages showed together with standard deviations.

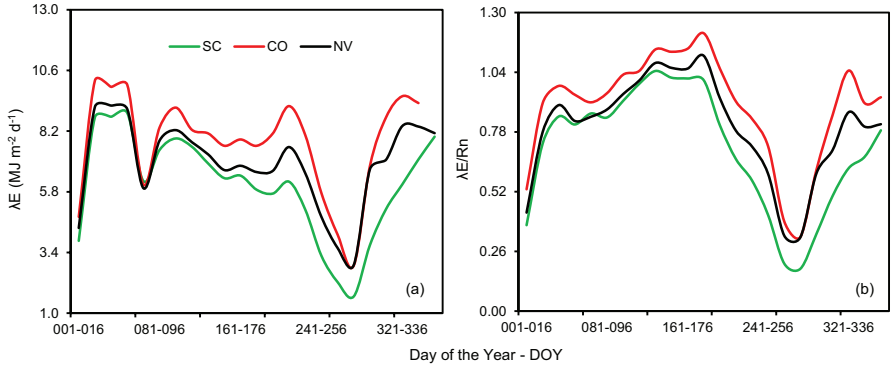

Figure 7. Average pixel values for the latent heat flux (λE) and their ratios to net radiation (Rn) for the sugarcane (SC), coffee (CO), and natural vegetation (NV) agroecosystems, during the year 2015, in the northeastern side of São Paulo (SP) state, Southeast Brazil.

Figure 7 presents the latent heat flux (λE) average values (a) and their fractions to Rn (b) for the sugarcane (SC), coffee (CO), and natural vegetation (NV) agroecosystems, during the year 2015.

Considering the three studied agroecosystems, the λE values started with short values, below 5.0 MJ m^{-2} d^{-1}, at the first half of January (2.0 mm d^{-1}), due to the low rainfall amounts (see **Figures 3a** and **7a**). After the first rains, λE followed the RG levels but dropping again in August because a short water scarcity spell. Clearly, one could see that in almost all periods of the year, for the coffee (CO) class, λE values were the highest ones, while for sugarcane (SC), they were the lowest ones. Natural vegetation (NV) presented intermediary λE values.

Energy balance differences among the agroecosystems were also noticed for the λE/Rn ratio. This last ratio is an index of the soil moisture in the root zones, and its behavior along the year evidenced two low-water availability periods in the root zones, with $\lambda E/R_n$ values below 0.60. One of these conditions was at the first half of January; however, for the sugarcane (SC) class, there was a longer period with low λE/Rn, from the first half of August to the end of October, dropping below 0.20.

Considering λE in terms of mm of waters, the evapotranspiration (ET) rates were from 0.7 to 3.6 mm d^{-1}, from 1.2 to 4.1 mm d^{-1}, and from 1.2 to 3.7 mm d^{-1} for the sugarcane (SC), coffee (CO), and natural vegetation (NV) agroecosystems, respectively. The corresponding annual average values were 2.5, 3.2, and 2.8 mm d^{-1}. Eksteen et al. [26] reported ET daily values for sugarcane (SC) between 1.6 and 2.9 mm d^{-1}, involving different varieties and soil moisture conditions, while in Florida (USA), Omary and Izuno [27] found a daily range from 0.7 to 4.6 mm d^{-1}. Regarding coffee (CO) crop, Vila Nova et al. [28] reported in Brazil, for the complete grain maturation, the mean ET rates of 3.5 mm d^{-1}, while Oliveira et al. [29] found an average of 2.9 mm d^{-1}. The ET values for the SC and CO agroecosystems in the current research are similar to these national and international studies.

The higher λE values for coffee (CO) than for sugarcane (SC) in the northeastern São Paulo state, Brazil, mean a larger annual water consumption for the first crop that should be considered under the conditions of water competition by agriculture and other sectors. Even with the cropland masks involving different stages of the agroecosystems in the current study, the similarity of our Rn and λE values with those from national and international literature provides confidence for the large-scale energy balance analyses by applying the SAFER algorithm throughout the MOD13Q1 product.

Considering the soil heat flux as a fraction of Rn, the sensible heat flux (H) was spatially retrieved by residue in the energy balance equation. The composed H values in sugarcane (SC), coffee (CO), and natural vegetation (NV) agroecosystems, during the year 2015 inside the northeastern side of São Paulo (SP) state, Southeast Brazil, are shown in **Figure 8**.

The sensible heat flux (H) values among the agroecosystems are also well differentiated according to the time of the year, but in this case with the highest values corresponding to the driest soil moisture conditions. They ranged from negative values as low as −3 MJ m^{-2} d^{-1} to high positive ones close to 13 MJ m^{-2} d^{-1}. The lowest ones were for the coffee (CO) class, which presented an average annual value of 0.6 ± 1.7 MJ m^{-2} d^{-1}, followed by natural vegetation (NV), 1.4 ± 1.8 MJ m^{-2} d^{-1}, and sugarcane (SC), with the highest average rate of 2.4 ± 2.2 MJ m^{-2} d^{-1}. Besides the highest H, the SC agroecosystem presented also the largest H spatial variation.

Taking into account all agroecosystem classes, the largest H values were during the driest conditions of the year, in the first half of January and from the second half of September to the end of October. The lowest ones, even negative, were at the end of the first rains, from April to the second half of July, when the root zones of the agroecosystems were moistier.

Figure 9 presents the H average values (a) and their fractions to Rn (b) for sugarcane (SC), coffee (CO), and natural vegetation (NV) agroecosystems, during the year 2015, in the north-eastern side of São Paulo (SP) state, Southeast Brazil.

In the middle of the year, negative H indicated horizontal heat advection from the drier and hotter natural areas to the wetter and colder cropped areas (**Figure 9a**). The highest positive

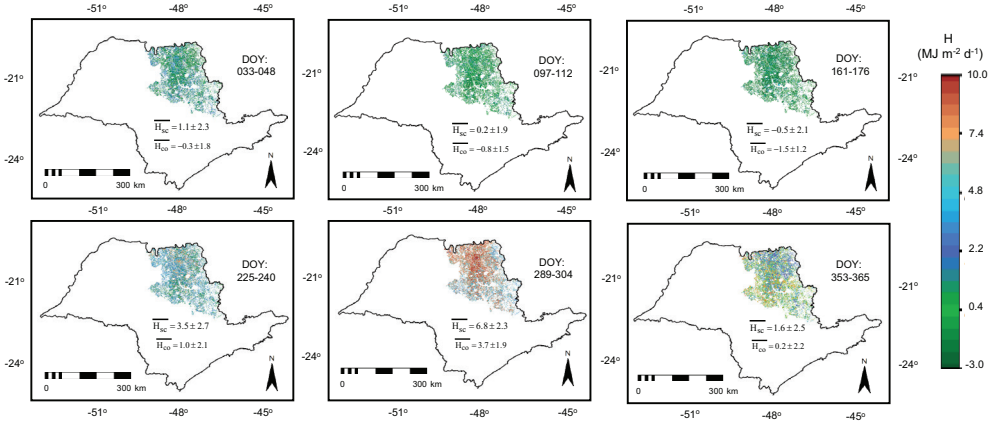

Figure 8. Composed sensible heat flux (H) values in sugarcane (SC), coffee (CO), and natural vegetation (NV) ecosystems, during the year 2015, inside the northeastern side of São Paulo (SP) state, Southeast Brazil. The over bars mean averages showed together with standard deviations (SD).

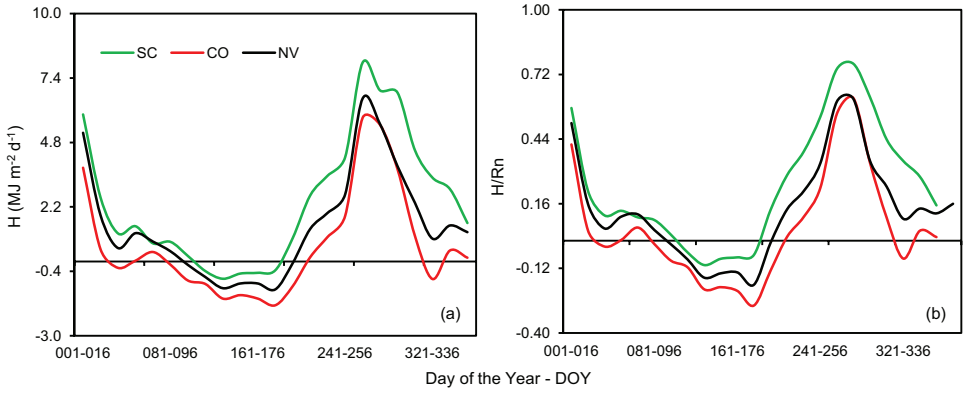

Figure 9. Average pixel values for the sensible heat flux (H) and their ratios to net radiation (Rn) in sugarcane (SC), coffee (CO), and natural vegetation (NV) ecosystems, during the year 2015, in the northeastern side of São Paulo (SP) state, Southeast Brazil.

values happened in the sugarcane (SC) class, reaching to the average of 8 MJ m^{-2} d^{-1} during the second half of September (DOY 257–252), when H represented 74% of Rn (**Figure 9b**). The lowest H values happened in the coffee (CO) class, during DOY 129–144, in May, when the average 16-day value was −1.5 MJ m^{-2} d^{-1}. During the year, the average annual H/Rn fractions were 0.07, 0.16, and 0.27 for coffee (CO), natural vegetation (NV), and sugarcane (SC), respectively. These results may represent cooling and warming microclimate effects as consequences of the replacement of the natural vegetation by coffee and sugarcane, respectively. Although sugarcane plants consume less water than the coffee ones, which is a positive aspect under the water scarcity conditions, the higher H rates for the sugarcane (SC) class have to be considered under the coupled effects of warming and land use change contexts.

Completing the energy balance, the composed ground heat flux (G) values in sugarcane (SC), coffee (CO), and natural vegetation (NV) agroecosystems, during the year 2015 inside the northeastern side of São Paulo (SP) state, Southeast Brazil, are shown in **Figure 10**.

Ground heat fluxes (G) among the agroecosystems are well distinct according to the time of the year, but with lower magnitudes than those for λE and H. The average pixel values ranged from 0.0 to 1.0 MJ m^{-2} d^{-1}. The spatial variations are low, with SD staying around 0.1 MJ m^{-2} d^{-1}. The average annual G values for sugarcane (SC) and coffee (CO) were the same (0.5 MJ m^{-2} d^{-1}), but for natural vegetation (NV), it was a little higher, with a mean value of 0.6 MJ m^{-2} d^{-1}.

Figure 11 presents the ground heat flux (G) daily average values (a) and their fractions to Rn (b) for sugarcane (SC), coffee (CO), and natural vegetation (NV) agroecosystems, during the year 2015.

The shapes of the curves pictured in **Figure 11** were somewhat similar of those for the latent heat flux (λE), but the values for the natural vegetation (NV) class moved from intermediary to the highest values. Lower G and of its ratio to net radiation (Rn) for the sugarcane (SC) class

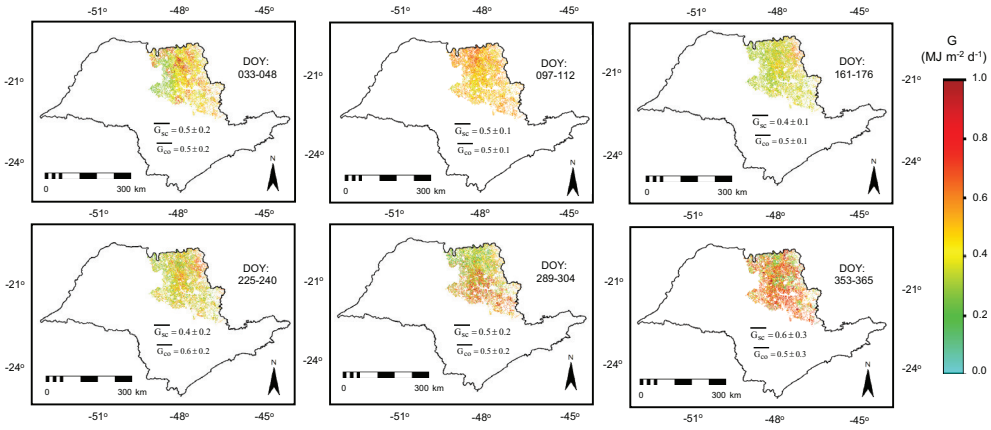

Figure 10. Composed ground heat flux (G) values for sugarcane (SC), coffee (CO), and natural vegetation (NV) agroecosystems, during the year 2015, inside the northeastern side of São Paulo (SP) state, Southeast Brazil. The over bars mean averages showed together with standard deviations.

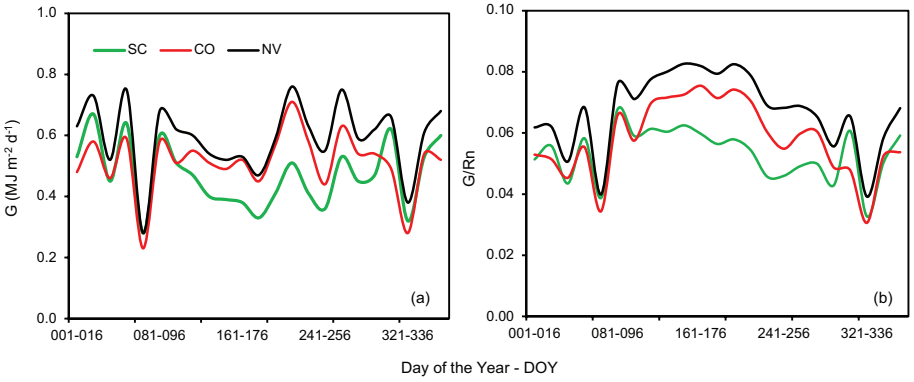

Figure 11. Ground heat flux (G) and their ratios to net radiation (Rn) in sugarcane (SC), coffee (CO), and natural vegetation (NV) agroecosystems, during the year 2015, in the northeastern side of São Paulo (SP) state, Southeast Brazil.

were found, mainly in the period of DOY 097–304 (April to the end of October). The average values of Rn partitioned as G were, respectively, 5, 6, and 7% for sugarcane (SC), coffee (CO), and natural vegetation (NV) agroecosystems.

4. Conclusions

The joint use of agrometeorological stations and the MODIS MOD13Q1 reflectance product allowed the large-scale energy balance quantification and analyses in the mixed agroecosystems composed by sugarcane, coffee, and natural vegetation along the year 2015 in the northeastern side of São Paulo state, Southeast Brazil. The strong dependence of net radiation (Rn) on the global solar radiation (RG) levels was clear for all classes, however, being lower for sugarcane and higher for coffee.

The daily values for the latent (λE), sensible (H), and ground (G) heat fluxes can be estimated in different kinds of vegetation from instantaneous measurements of the reflectances from the MODIS sensor, throughout the application of the SAFER algorithm. The lowest and the highest λE were, respectively, for sugarcane and coffee. Although sugarcane presents lower evapotranspiration rates than coffee crop in an annual scale, being a positive aspect under the actual water scarcity conditions, its higher H has to be considered under the conditions of the coupled effects of warming and land use changes.

Acknowledgements

The authors acknowledge the National Council for Scientific and Technological Development (CNPq) for the financial support to a project on large-scale radiation and energy balances in Brazil.

Author details

Antônio Heriberto de Castro Teixeira[1]*, Janice F. Leivas[2], Carlos C. Ronquim[2] and Gustavo Bayma-Silva[2]

*Address all correspondence to: heriberto.teixeira@embrapa.br

1 Embrapa Coastal Tablelands, Aracaju-SE, Brazil

2 Embrapa Satellite Monitoring, Campinas-SP, Brazil

References

[1] Satolo LF, Bacchi MRP. Impacts of the recent expansion of the sugarcane sector on municipal per per capita income in São Paulo state. ISRN Economics. 2013;**2013**:1-14. http://dx.doi.org/10.1155/2013/828169

[2] Mello CO, Esperancini MST. Análise econômica da eficiência da produção de cana-de-açúcar de fornecedores do Estado do Paraná. Revista Energia na Agricultura. 2012;**27**:48-60. http://dx.doi.org/10.17224/EnergAgric.2012v27n3p48-60s

[3] Rudorf BFT, Aguiar DA, Silva WF, Sugawara LM, Adami M, Moreira MA. Studies on the rapid expansion of sugarcane for ethanol production in São Paulo state (Brazil) using Landsat data. Remote Sensing. 2010;**2**:1057-1076. DOI: 10.3390/rs2041057

[4] Scharlemann JP, Laurance WF. How green are biofuels? Science. 2008;**319**:43-44. DOI: 10.1126/science.1153103

[5] Waclawovsky AJ, Sato PM, Lembke CG, Moore PH, Souza GM. Sugarcane for bioenergy production: An assessment of yield and regulation of sucrose content. Plant Biotechnology Journal. 2010;**8**:1-14. DOI: 10.1111/j.1467-7652.2009.00491.x

[6] Chooyok P, Pumijumnog N, Ussawarujikulchai AT. The water footprint assessment of ethanol production from molasses in Kanchanaburi and Supanburi province of Thailand. Procedia APCBEE. 2013;**5**:283-287. http://dx.doi.org/10.1016/j.apcbee.2013.05.049

[7] Beringer T, Lucht W, Schaphoff S. Bioenergy production potential of global biomass plantations under environmental and agricultural constraints. GCB Bioenergy. 2011;**3**:299-312. http://dx.doi.org/10.1111/j.1757-1707.2010.01088.x

[8] Cerri CC, Galdos MV, Maia SMF, Bernoux M, Feigl BJ, Powlson D, Cerri CEP. Effect of sugarcane harvesting systems on soil carbon stocks in Brazil: An examination of existing data. European Journal of Soil Science. 2011;**62**:23-28. http://dx.doi.org/10.1111/j.1365-2389.2010.01315.x

[9] Anderson-Teixeira KJ, Snyder PK, Twine TE, Cuadra SV, Costa MH, de Lucia EH. Climate-regulation services of natural and agricultural ecoregions of the Americas. Nature Climate Change 2012;**2**:177-181. http://dx.doi.org/10.1038/nclimate1346

[10] Teixeira AH de C, Hernandez FBT, Scherer-Warren M, Andtrade RG, Victoria D de C, Bolfe EL, Thenkabail PS, Franco RAM. Water productivity studies from earth observation data: Characterization, modeling, and mapping water use and water productivity. In: Prasad ST, editor. Remote Sensing of Water Resources, Disasters, and Urban Studies. 1st ed. Vol. III. Boca Raton: Taylor and Francis; 2015, pp. 101-126. ISBN 9781482217919

[11] Teixeira AH de C, Bastiaanssen WGM, Ahmad M–u–D, Bos MG, Moura MSB. Analysis of energy fluxes and vegetation-atmosphere parameters in irrigated and natural ecosystems of semi-arid Brazil. Journal of Hydrology. 2008;**362**:110-127. http://dx.doi.org/10.1016/j.jhydrol.2008.08.01

[12] Teixeira AH de C. Determining regional actual evapotranspiration of irrigated and natural vegetation in the São Francisco river basin (Brazil) using remote sensing and Penman-Monteith equation. Remote Sensing. 2010;**2**:1287-1319. DOI: 10.3390/RS0251287

[13] Cabral OMR, Rocha HR, Gash JH, Ligo MAV, Ramos NP, Packer AP, Batista ER. Fluxes of CO_2 above a sugarcane plantation in Brazil. Agricultural and Forest Meteorology. 2013;**182-183**:54-56. http://dx.doi.org/j.agrformet.2013.08.004

[14] da Silva TGF, Moura MSB, Zolnier S, Soares JM, Vieira VJ de S, Júnior WFG. Demanda hídrica eficiência do uso da água da cana-de-açúcar irrigada no semiárido brasileiro. Revista Brasileira de Engenharia Agrícola e Ambiental. 2011;**15**:1257-1265. http://dx.doi.org/10.1590/1807-1929/agriambi.v19n9p849-856

[15] Tejera NA, Rodes R, Ortega E, Campos R, Lluch C. Comparative analysis of physiological characteristics and yield components in sugarcane cultivars. Field Crops Research. 2007;**102**:64-72. http://dx.doi.org/10.1016/j.fcr.2007.02.002

[16] Camargo AP. Zoneamento de aptidão climática para a cafeicultura de arábica e robusta no Brasil. In: Fundação IBGE, Recursos, meio ambiente e poluição. 1977. pp. 68-76

[17] Camargo AP, Camargo MBP. Definição e esquematização das fases do cafeeiro arábica nas condições tropicais do Brasil. Bragantia. 2001;**60**:65-68. http://dx.doi.org/10.1590/S0006-87052001000100008

[18] Júnior AFC, Júnior OA de C, Martins E de S, Guerra AF. Phenological characterization of coffee crop (*Coffea arabica* L.) from MODIS time series. Revista Brasileira de Geofísica. 2013;**31**:569-578. http://dx.doi.org/10.22564/rbgf.v31i4.338

[19] Allen RG, Pereira LS, Raes D, Smith M. Crop Evapotranspiration: Guidelines for Computing Crop Water Requirements. Rome: Food and Agriculture Organization of the United Nations; 1998. p. 300

[20] Valiente JA, Nunez M, Lopez-Baeza E, Moreno JF. Narrow-band to broad-band conversion for Meteosat-visible channel and broad-band albedo using both AVHRR-1 and -2 channels. International Journal of Remote Sensing. 1995;**16**:1147-1166. http://dx.doi.org/10.1080/01431169508954468

[21] Teixeira AH de C, Leivas JF, Hernandez FBT, Franco RAM. Large-scale radiation and energy balances with Landsat 8 images and agrometeorological data in the Brazilian semiarid region. Journal of Applied Remote Sensing. 2017;**11**:016030. http://dx.doi.org/10.1117/1.JRS.11.016030

[22] Teixeira AH de C, Leivas JF, Silva GB. Options for using Landsat and RapidEye satellite images aiming the water productivity assessments in mixed agro-ecosystems. Proceedings of SPIE. 2016;**9998**:99980A-1-99980A-11. DOI: 10.1117/12.2240119

[23] Inman-Bamber NG, Smith D. Water relations in sugarcane and response to water deficits. Field Crops Research. 2005;**92**:185-202. http://dx.doi.org/10.1016/j.fcr.2005.01.023

[24] Hughes CE, Kalma JD, Binning P, Willgoose GR, Vertzonis M. Estimating evapotranspiration for a temperate salt marsh Newcastle, Australia. Hydrological Processes. 2001;**15**:957-975. http://dx.doi.org/10.1016/j.fcr.2005.01.023

[25] Yunusa IAM, Walker RR, Lu P. Evapotranspiration components from energy balance, sapflow and microlysimetry techniques for an irrigated vineyard in inland Australia. Agricultural and Forest Meteorology. 2004;**127**:93-107. http://dx.doi.org/10.1016/j.agrformet.2004.07.001

[26] Eksteen A, Singels A, Ngxaliwe S. Water relations of two contrasting sugarcane genotypes. Field Crops Research. 2014;**168**:86-100. http://dx.doi.org/10.1016/j.fcr.2014.08.008

[27] Omary M, Izuno FT. Evaluation of sugar-cane evapotranspiration from water table data in the everglades agricultural area. Agricultural Water Management. 1995;**27**:309-319. http://dx.doi.org/10.1016/0378-3774(95)01149-D

[28] Villa Nova NA, Favarin JL, Angelocci LR, Dourado Neto D. Estimativa do coeficiente de cultura do cafeeiro em função de variáveis climatológicas e fitotécnicas. Bragantia. 2002;**61**:81-88. http://dx.doi.org/10.1590/S0006-87052002000100013

[29] Oliveira PM, Silva AM, Castro Neto P. Estimativa da evapotranspiração e do coeficiente de cultura do cafeeiro (*Coffea arabica* L.). Irriga. 2003;**8**:273-282 ISSN: 1808-8546